



Factors influencing the extent and development of the oxic zone in sediments

WILLIAM A. HOUSE

Centre for Ecology and hydrology, Winfrith Technology Centre, Dorchester, DT2 8ZD, Dorset, UK (e-mail: wah@ceh.ac.uk)

Received 6 March 2002; accepted in revised form 28 March 2002

Key words: Oxygen, Sediment oxygen demand, Sediment-water interface, Sediments

Abstract. Dissolved oxygen concentrations in river-sediment porewaters are reported and modelled using a zero-order reaction rate and the Monod equation. After mixing the sediments and allowing settling, the dissolved oxygen profile in the bed-sediment was expected to reach a steady-state rapidly (< 1 h). However changes in the vertical profile of oxygen over a period of 38 days revealed that the penetration of oxygen increased and the dissolved oxygen flux at the interface decreased with time, probably as the oxidation kinetics of organic matter and redox reactions in the sediment changed. Experiments with three contrasting silt and sand dominated sediments (organic matter content between 0.9 and 18%) at two water velocities (*ca* 10 and 20 cm s⁻¹) showed that the dissolved oxygen profiles were independent of velocity for each of the sediments. The most important controls on the reaction rate were the organic matter content and specific surface area of the sediment. A viscous diffuse-boundary-layer above the sediment was only detected in the experiments with the silt sediment where the sediment oxygen demand was relatively high. In the coarser sediments, the absence of a diffuse layer indicated that slow oxidation processes in the sediment controlled the dissolved oxygen flux at the interface. The problem of determining a surface reference in coarse sediment is highlighted. The results are discussed with reference to other studies including those concerned with estuarine and marine sediments.

Introduction

The oxygen concentration in sediment porewaters is an important control on a number of chemical and biological processes including those influenced by trace metal speciation, e.g. Fe²⁺/Fe³⁺ transformation, the solubility of minerals, e.g. vivianite, Fe₃(PO₄)₂ and denitrification (Nielson et al. 1990). The dissolution of solid solutions of iron hydroxide/phosphate during oxic to anoxic transformations is known to be an important mechanism controlling the release of inorganic phosphate from minerals to porewater in some lake sediments (Wersin et al. 1991) and precipitation of vivianite in anoxic conditions influences soluble phosphorus concentrations in sediment porewaters (Nriagu and Dell 1974; Woodruff et al. 1999). The extent of the penetration of oxygen in sediments also influences the structure and distribution of benthic communities (Llanso 1992). Although less information is available about the effects of oxygen on transformations of trace organic contaminants, e.g. pesticides, many types of compound degrade more slowly below

the oxic zone of bed-sediments, and are therefore persistent once they are buried. For example, a pronounced redox effect has been shown for both herbicides, mecoprop and MCPA (2-methyl-4-chlorophenoxy acetic acid). As the oxygen concentration decreased, transformation rates decreased by approximately 170 fold over a period of 200 days (Vink and Van der Zee 1977).

As well as the direct effects on processes in aquatic sediments, the flux of oxygen across the water-sediment interface partly controls the concentration of oxygen in the overlying water. The determination of the Sediment Oxygen Demand, SOD, has been the focus of many studies in both fresh water and marine systems, e.g. Edwards and Rolley (1965) and Pamatmat and Banse (1969), Bowman and Delfino (1980), Barcelona (1983), Park and Jaffe (1999). However many of the methods are not well suited to applications in lotic systems where the flow of water at the interface may influence dissolved oxygen transport (Berninger and Markus 1997; Mackenthun and Stefan 1998; Josiam and Stefan 1999) and determines the SOD and penetration of oxygen into the sediment. Depending on the residence time of the overlying water, the flux of oxygen through the interface will influence the dissolved oxygen concentration in the water. If the sediment is disturbed, the mixing of anoxic porewaters and suspended sediment of potentially high oxygen demand, may lead to the depletion of oxygen in the bulk water and associated adverse effects (Jubb et al. 2001).

The present work focuses on the oxygen penetration into soft-sediments without photosynthesising biofilms and in relatively fast flowing waters chosen to reflect the hydrodynamics conditions in rivers. Because of the difficulties of measuring SOD in systems open to the atmosphere, the penetration of oxygen into the sediment is measured using oxygen microelectrodes (Revsbech et al. 1980) with the sediments contained in a fluvium channel. Vertical profiles in dissolved oxygen (DO) concentration through the sediment porewater are modelled to obtain reaction rate constants and DO fluxes at the interface. The effects of the exposure time, river sediment composition and water velocity above the sediment are investigated to provide an insight into the conditions controlling DO penetration.

Methods

Fluvium channel experiments

Fluvium channels of a design similar to that of House et al. (1995) were used (see Figure 1). The sediment bed was approximately 2 m in length and 10 cm wide. The solution was mixed in an entrance tank prior to passing over the sediment. In all the experiments the sediments were covered to exclude light, apart from when the dissolved oxygen profiles were being measured. River bed-sediments were collected from surface sediments (< 5 cm depth) at various river sites (see Table 1), sieved to 2 mm size, well mixed, and placed in stainless steel trays of dimension 40 × 10 × 5 cm. The surface of the sediment was levelled to the top of the trays

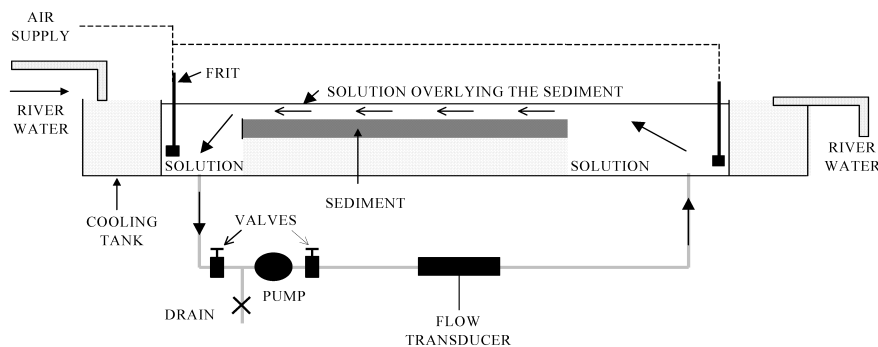


Figure 1. Schematic of the fluvium channel showing the pump, control valve and aeration equipment. The sediment and overlying water are contained in an acrylic channel surrounded by river water.

and the trays placed in a fluvium channel constructed of acrylic plastic (Figure 1). Twenty litres of river water from the River Frome were carefully placed in the channel to give a depth of water overlying the sediment of approximately 3 cm. The water was continually aerated to maintain DO saturation and recirculated over the sediment at a velocity controlled by a butterfly valve placed after the pump and monitored using a flow transducer. The bulk water velocity over the sediment was calculated from the flow rate in the pump circuit and checked dye tracer measurements at the end of the experiment. The temperature of the sediment was controlled by circulating water from the nearby River Frome around the outside of the fluvium channel. This ensured that natural diurnal changes in temperature were followed throughout the experiment. At the end of the experiment, the sediment was sectioned to obtain material for characterisation, e.g. porosity, organic matter and particle density measurements. This was achieved by draining the excess water from the channel to the level of the sediment surface, and sectioning longitudinally at 1 mm intervals using a tool designed to collect both the porewater and sediment. The tool consisted of a knife-edge and collection chamber supported on runners that were fixed to the sides of the channel. The depth of the knife-edge was adjusted by screw threads allowing precise positioning of the cutting edge relative to the sediment surface. The water content and porosity were measured by weighing after drying at 105 °C overnight and the organic matter after combustion at 550 °C overnight. The specific surface area of the selected sediment was measured by gas adsorption (outgassed for 16 h at 60 °C) using a Beckman/Coulter SA3100 and BET analysis. X-ray diffraction of the sediment was done using a Philips PW 1380 horizontal goniometer with 1710 diffraction control. The particle-size was determined by sedimentation.

Microelectrode measurements

Dissolved oxygen concentrations in the sediment porewaters were measured using a microelectrode based on the Clark design with a guard cathode (Diamond General corp., Michigan, USA) and used previously for measurements in lake sediments

Table 1. Sediments used in the experiments. Key: OM is % organic matter by mass. Size fractions: clay < 2 μm ; silt 2–63 μm and sand 63–850 μm .

Code	River	NGR	Dominant size fraction	Reference	OM
A	Blackwater	SU885538	Silt	(House et al. 2000)	11.3
B	Calder	SE409258	Silt	(Allan et al. 2001)	6–6.5
C	Frome	SY872887	Sand	Thirkette and Barrett (1994)	0.9
D	Frome	SY871868	Silt	Thirkette and Barrett (1994)	16.7
E	Frome	–	Mixture C+D		5.0

(Martin et al. 1993). The microelectrode was connected to a picoammeter (Keithley) and polarisation voltage adjusted to 750 mV. The current drift was typically < 2% h^{-1} and response time of 90% of signal in < 4 s. The microelectrode profiles through the bulk water, water-sediment interface and sediment in the channel were measured automatically using a Visual Basic computer program. The analogue output from the ammeter was interfaced to the computer and the position of the electrode was controlled by a stepper-motor connected to the computer giving a depth resolution for the electrode of 13 μm . The first movement of a sediment particle on vibrating the electrode was taken as the surface. The electrode was calibrated during each vertical profile by firstly noting the signal in the bulk water (nominally 100% saturation as the water was aerated once the sediment was placed in the channel). The actual DO concentration was measured using a conventional Clark electrode (Mettler-Toledo) pre-calibrated at 100% saturation and with sodium sulphite solution. When the electrode was in the sediment and the signal was independent of depth, the zero concentration calibration point was determined. The water temperature, atmospheric pressure and temperature during the profile measurement were noted and used to calculate the DO concentration using the equation given by Benson and Krause (1980) with corrections for water vapour pressure. Initial experiments with darkened sediments left in the channel for several weeks, indicated that profiles of DO through the sediment at different locations along the channel were similar with no systematic changes at the interface discernible.

Experiments

Two main experiments were performed using the bed-sediments described in Table 1. The first experiment with Sediment A was to investigate the application of the models describing concentration changes in the sediment with depth, and also the temporal changes in oxygen penetration. This involved measuring 30 profiles of DO over a period of 38 days. The second experiment was designed to investigate the effects of sediment composition and water flow on the DO penetration. Three sediments of different organic matter content were used. Two were in contrasting sediments from the same location, one a river sand (sediment C) and the other a fine silt (sediment D). A third sediment (sediment E) was made of an approximately equivolume mixture of the sediments C and D. Triplicate profiles of

DO concentration through the sediments were made at velocities of 10 cm s^{-1} at 15 days after mixing and at 20 cm s^{-1} at 28 days after mixing. Higher velocities could not be used because of the resuspension of bed-sediment. As all sediments were only sieved to 2 mm size, some benthic animals, mainly *oligochaete* worms, were included. The effects of these were checked in an ancillary experiment with Sediment B. The sediment was well mixed before use and placed in two fluvarium channels in the dark. The channels developed different worm densities that were measured at the end of the experiment by removing a 10 cm section to a depth of 4 cm of sediment for sieving. After 5-weeks, profiles of DO concentration at three different locations were made in each channel.

Theory

The diffusion of dissolved oxygen into sediment may be described by the differential equation:

$$dc(x)/dt = D_s[d^2c(x)/dx^2] - g \quad (1)$$

subject to the boundary conditions $c(x) = c_0$ at $x = 0$ for $t \geq 0$ and where D_s is the diffusion coefficient of oxygen in the sediment, c is the concentration of dissolved oxygen in the porewater, x is the distance from the water-sediment interface and $g(x)$ is a function describing the net reaction of dissolved oxygen in the porewater. No attempt is made here to distinguish the various reactions that contribute to the function g but they include both biochemical reactions involving the oxidation of organic matter by microbes and chemical redox reactions.

The diffusion coefficient of oxygen in sediments may be estimated from the porosity of the sediment from the relationship (Boudreau 1997):

$$D_s = D_m/(1.0 - \ln\phi^2) \quad (2)$$

where D_m is the molecular diffusion coefficient of oxygen in water and ϕ is the sediment porosity. The diffusion coefficient, D_m , was taken from the temperature relationship given by (Han and Bartels 1996):

$$\text{Log}_{10}(D_m) = -4.410 + 773.8/T - (506.4/T)^2 \quad (3)$$

where D_m is in $\text{cm}^2 \text{ s}^{-1}$.

Several equations have been used to describe the reaction of oxygen in the sediment porewater, including:

- (a) First-order reaction kinetics.

$$g(x) = k_1c(x) \quad (4)$$

where k_1 is the first-order rate constant.

- (b) Zero-order kinetics.

$$g = k_0 x_f \quad (5)$$

where $x_f = \rho_{\text{sed}}(1-\phi)$ is the dry mass of sediment in unit volume of wet sediment, k_0 is the zero-order rate constant, ρ_{sed} the density of sediment particles and ϕ the sediment porosity.

- (c) Monod equation.

$$g(x) = x_f [k_b c(x) / (c(x) + k_c)] \quad (6)$$

where k_b and k_c are constants. If $k_c \ll c(x)$ then $k_b = k_0$ in equation (5).

- (d) Combined first and zero order.

$$g = k_0 x_f \quad \text{for } c > c_1 \quad (7)$$

$$g(x) = k_1 c(x) \quad \text{for } c < c_1 \quad (8)$$

where c_1 is the transition point from zero-order to first-order kinetics typically equated with 5% saturation of dissolve oxygen.

Equation (1) was solved numerically using the method of lines with the solution represented by cubic Hermite polynomials (Sincovec and Madsen 1975). The values of k_1 , k_0 , k_b and k_c describing the reaction function (g) were determined numerically by either iteration (for Equations (4) and (5)) or a Simplex algorithm for two parameter functions. The optimisation of the rate constant was achieved by minimising the root-mean-square of the deviations between the calculated and experimental data. The experimental data of the variation of the oxygen concentration with depth were selected from the surface to a maximum depth where $c(x) = 0$ and fitted using cubic splines so that 20 equidistant data points were interpolated within the interval. The oxygen flux was calculated by Fick's First Law from the best fit of the model using 5 points nearest to the interface. The penetration depth of oxygen (δ) was determined as the distance from the interface to the depth at which the DO concentration reached zero.

The results using Equation (5) were found to agree with the steady-state limit Bouldin (1968):

$$c(x) = Ax^2/sD_s - (2c_0A/D_s)^{1/2}x + c_0 \quad (9)$$

where $c(x) = c_0$ at $x = 0$ and A is a rate constant in units of $\mu\text{mol dm}^{-3} \text{ s}^{-1}$. If $c(x)$ is in $\mu\text{mol dm}^{-3}$ then the first-order rate constant may be written:

$$k_0 = A/[\rho_{\text{sed}}(1-\phi)] \quad (10)$$

in $\mu\text{mol kg}^{-1} \text{ s}^{-1}$. Also with this model and steady-state limit, the penetration depth

of oxygen may be written as (Cae and Sayles 1996):

$$\delta = 2\phi D_{s,c_0}/F^0 \quad (11)$$

where F^0 is the DO flux at $x = 0$ calculated from:

$$F^0 = -\phi D_{s,c} dc(x)/dx$$

Results and discussion

Investigation of the temporal changes in oxygen penetration

These experiments were with Sediment A from the River Blackwater (Table 1). This relatively small lowland river is on the county boundary between Surrey and Hampshire, accumulates fine organic rich sediment in several reaches and is heavily impacted by treated sewage effluent. The sediment was composed of a mixture of quartz (69%), vivianite (22%), calcite (3%), dolomite (3%) and clay (3%). The clay was dominated by illite (38%), expandable clays (45%) and kaolinite (17%). The particle size distribution was dominated by the 68% silt fraction, with 21% sand and 11% clay. The specific surface area was found to be $8.4 \text{ m}^2 \text{ s}^{-1}$.

The sediment was placed directly in the fluvium channel. The mean temperature during the measurements over 38 days was $18.4 \text{ }^\circ\text{C}$ with a range of 18.0 to $19.3 \text{ }^\circ\text{C}$. The mean pH of the water was 8.28 with a range of 8.00 to 8.60 . The mean temperature on the day of the measurements was used in the modelling (see Table 2) and no account was taken of the natural diurnal changes. The overlying water was aerated at all times.

Examples of the changes in DO concentration profiles measured from the sediment – water interface to the point where the DO concentration was zero, are shown in Figure 2a. During the first day, the penetration of DO was $\approx 1 \text{ mm}$ (see Table 2) and thereafter this increased to reach almost 3 mm after 38 days (Figure 2a). On chosen days throughout the experiment, replica profiles were completed at different positions on the bed. The data from the microelectrode profiles made in replica on the same day, i.e. days zero, 1, 2, 7, 14 and 37–38 from the start as collated in Table 2, were analysed numerically as described above with $\rho_{\text{sed}} = 2.7 \text{ ml g}^{-1}$ and porosity of 0.80 . The root-mean-square (rms) deviations were consistently higher for the first-order optimisations by a factor of approximately 2. Better agreement was found with the combined first and zero-order equation although the optimisation was not very sensitive to the first-order rate constant and gave similar rms values to the zero-order function alone, e.g. the last profile gave a $k_0 = 0.08 \text{ } \mu\text{mol kg}^{-1} \text{ s}^{-1}$ and $k_1 = 0.0051 \text{ s}^{-1}$ and rms of 6 which compared with a value of $k_0 = 0.13 \text{ } \mu\text{mol kg}^{-1} \text{ s}^{-1}$ and rms of 7 for the zero-order function alone. The other two-parameter function, the Monod equation, produced good agreement with the

Table 2. Temporal changes in dissolved oxygen penetration into sediment A over a period of 38 days. k_0 is the zero-order rate constant unless otherwise denoted, and rms is the root-mean-square deviation between the model prediction and the experimental dissolved oxygen profiles. For values listed with *, the Monod equation gave the best fit with k_b listed as k_0 and $k_c = 0.06, 0.10$ and $0.13 \mu \text{ mol dm}^{-3}$ for the first three profiles.

Time/d	Mean temp./°C	$k_0/\mu\text{mol kg}^{-1} \text{ s}^{-1}$	rms/ $\mu\text{mol dm}^{-3}$	Flux/nmol $\text{m}^{-2} \text{ s}^{-1}$	Penetration depth/mm
0.06	20.1	4.67*	24	985	0.98
0.17	18.9	0.88*	7	470	1.25
0.32	18.9	1.74*	14	677	0.93
1.10	18.6	1.79	13	690	0.74
1.19	19.1	1.33	13	583	1.06
1.28	19.3	1.03	11	525	1.20
2.07	18.7	0.52	18	367	1.64
2.42	18.5	0.51	12	368	1.55
7.05	18.2	0.26	13	256	2.34
7.20	18.6	0.24	22	243	2.37
7.30	18.6	0.22	9	239	2.40
14.07	18.9	0.44	11	332	1.93
14.19	19.3	0.26	10	254	2.20
37.20	18.7	0.18	13	210	2.77
38.25	18.7	0.13	7	187	2.53

experimental data, especially for the profiles measured on the first day. The k_b values calculated for the Monod function were close to the corresponding k_0 values and the solution was generally insensitive to the choice of k_c (Equation 6). The rms values after the first day were similar to those from the optimisation with the zero-order function. Hence for the majority of the analysis the zero-order solution was used to describe the DO profiles.

The results of calculations using the Monod or zero-order rate functions, indicate a large decrease in the reaction during the first 7 days (Figure 2b and Table 2) corresponding to an increase in the penetration depth (Figure 3a) and five-fold decrease in the DO flux across the interface (Figure 3b). The time to reach a steady-state DO profile for the experimental conditions and with $k_0 = 1 \mu \text{mol kg}^{-1} \text{ s}^{-1}$ was examined and found to be < 60 min (Figure 4). This is in general agreement with the experimental results obtained by (Revsbech et al. 1980) for profiles in marine sediments with photosynthetic organisms; the steady-state was achieved after 30 mins at 10°C and < 10 min at 18°C . As the temperature changes during the experiment were relatively small (Table 2), changes in SOD had to be caused by other factors such as a decrease in porosity of the sediment as particles initially settled in the bed, and changes in the microbial community or oxidation processes that occurred during the experiment. Simulations of DO profiles that developed over 1 hour for different sediment porosities showed that the depth of penetration of oxy-

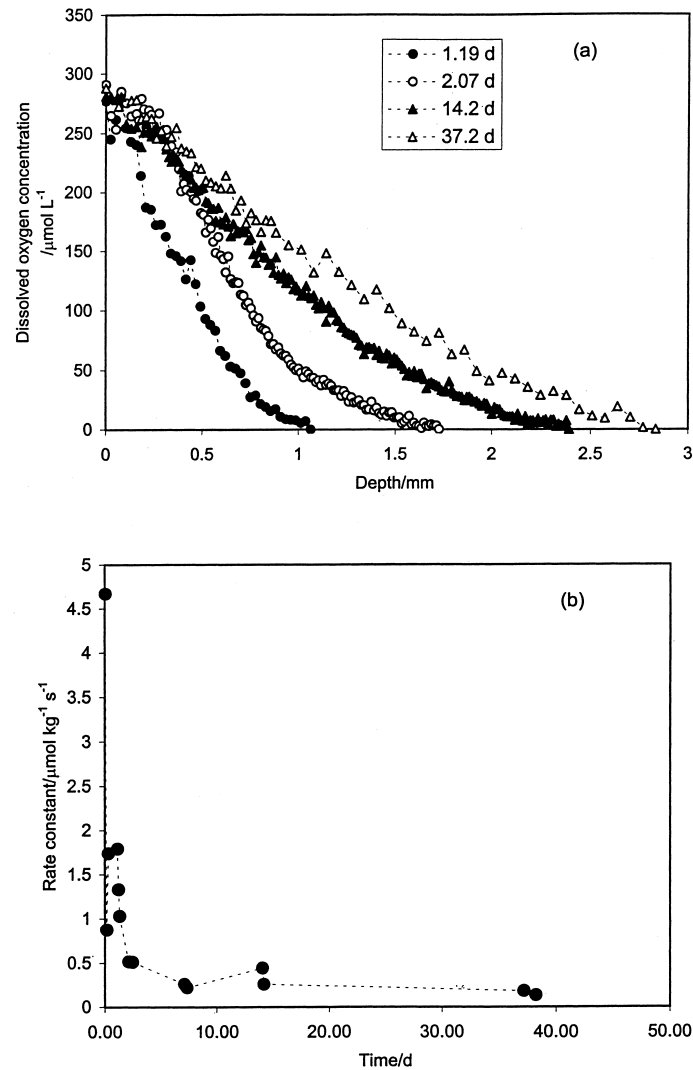


Figure 2. Results of the investigation of temporal changes in dissolved oxygen movement in Sediment A. (a) Changes in the measured dissolved oxygen concentration profile with time. (b) Variations in the oxidation rate constant during the experiment.

gen decreased as the porosity was reduced and therefore cannot explain the trend shown in Figure 3a.

As the steady-state profile is achieved rapidly in these experiments, it is possible to test the relationship of (Cae and Sayles 1996). This model assumes zero-order kinetics, a steady-state profile, a uniform reaction of oxygen through the profile and negligible porewater irrigation. The rate constant, A , calculated from Equation (9) agreed with k_0 (Equation 5). The relationship between the penetration depth and

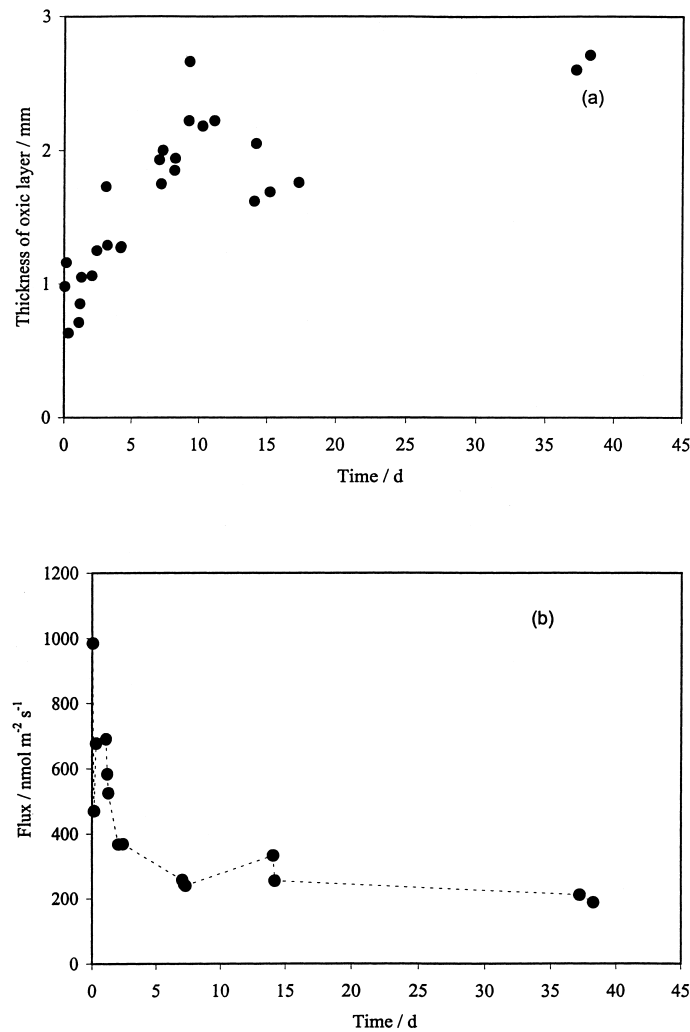


Figure 3. Results from the analysis of the temporal changes. (a) Trend in the increase in thickness of the oxic layer during the experiment. (b) Changes in the dissolved oxygen flux at the interface.

the inverse of the DO flux at the interface (Table 2) was linear ($R^2 = 0.92$) as shown in Figure 5a with a slope of $568 \pm 16 \text{ nmol m}^{-1} \text{ s}^{-1}$ which is close to the predicted value of $664 \text{ nmol m}^{-1} \text{ s}^{-1}$ from Equation (11). This equation has been found to be valid for continental margin marine sediments (where penetration depths are several centimetres) (Cae and Sayles 1996). The results obtained here support the proposition by Cae and Sayles (1996), that the model can be used to describe small scale (mm depth) DO penetration depths typical of organic rich sediments.

The ancillary experiment to investigate the effects of low densities of *oligochaete* worms also gave good agreement with the zero-order model with the rate con-

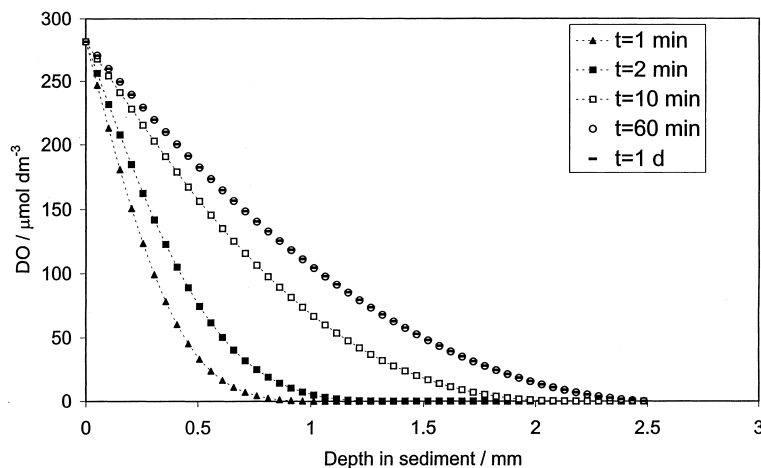


Figure 4. Theoretical dissolved oxygen concentration profiles generated for Sediment A with $k_0 = 1 \mu\text{mol kg}^{-1} \text{s}^{-1}$ as steady-state is approached.

starts in the two channels of 0.044 (0.003 SD) $\mu\text{mol kg}^{-1} \text{s}^{-1}$, and 0.039 (0.003 SD) $\mu\text{mol kg}^{-1} \text{s}^{-1}$ for worm densities of *ca.* 200 m^{-2} and 1200 m^{-2} . These were mainly *Limnodrilus* ssp. and *Potamothrix* ssp. with some *Tubifex* ssp. of 1–2 cm in length. At relatively low densities, no effects on the DO flux could be established with values of 100 (5 SD) and 109 (4 SD) $\text{nmol m}^{-2} \text{s}^{-1}$ (SD: Standard Deviation) for the low and high densities respectively. Although the respiration of animals certainly affects the SOD of river sediments (Edwards and Rolley 1965), this is not reflected in the DO concentration profiles, as the effects are likely to be localised to the immediate vicinity of the burrows.

Effects of water velocity and sediment composition

These experiments were performed with sediments C, D and E. Sediment C was dominated by a sand fraction (95%) with silt (4.6%) and clay (0.4%) whereas Sediment D was dominated by a silt fraction (51%) with sand (15%) and clay (34%). The DO profiles were measured several days after mixing to ensure that changes in the profile were relatively slow (Figure 2b). The pH of the overlying water was 8.34 ± 0.07 ($n = 7$) at the time of measurement, the DO was $100 \pm 2\%$ ($n = 7$) and temperature was 8.6°C at the lower flow velocity (adjusted to 10 cm s^{-1}) and 12.7°C at the higher flow velocity (adjusted to 20 cm s^{-1}) although differences in the sediment temperature during the measurements was expected to be less than this.

The results from the analysis of the DO profiles for the three sediments obtained at two flow velocities are given in Table 3, and the characteristics of the surface sediments obtained at the end of the experiments after longitudinally sectioning the sediment, in Table 4. There was a good correlation ($R^2 = 0.94$) between the rate constant from the steady-state model and the numerical solution based on the zero-order function. The rms values (Table 3) are of similar magnitude to those in Table 2

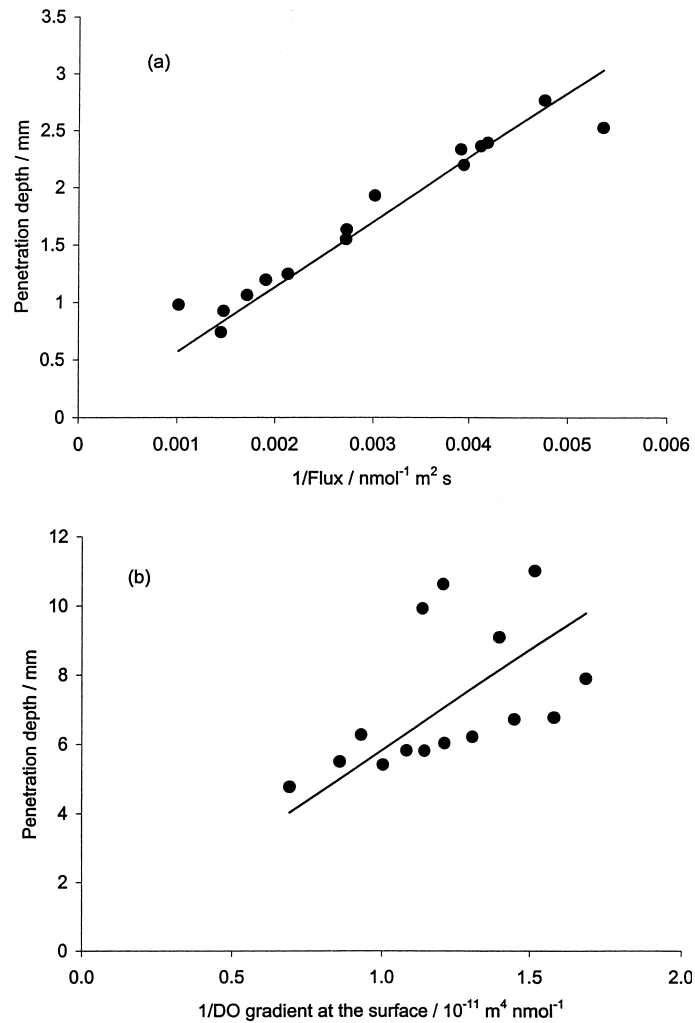


Figure 5. Regression relationships obtained according to Equation (11). (a) Sediment A, $R^2 = 0.92$. (b) Sediments C, D and E, $R^2 = 0.30$.

and the DO fluxes are lower, even for the organic rich sediment, D, probably as a result of the differences in temperature of the two experiments (Edwards and Rolley 1965). For example, Chen et al. (1999) observed an approximate doubling in SOD between 11 and 18 °C for a tidal river sediment. The sediments cover a range of properties typical of river sediments (Table 4).

An analysis of the zero-order rate constants obtained for each sediment type in the two flow conditions, failed to show any significant differences caused by velocity (t-test with a Confidence Level, CL, 95%). The same remained true when the data for each series were corrected to 20 °C using the relationship of Seiki et al.

Table 3. Results of microelectrode measurements of oxygen penetration into three different sediments. **Key:** Low, low velocity (10 cm s⁻¹); High, high velocity (20 cm s⁻¹); DBL, rms, root-mean-square deviation between experimental DO profiles and calculated.

Sediment code	Velocity category	A/10 ⁻³ μmol dm ⁻³ s ⁻¹	k _o /10 ⁻² μmol kg ⁻¹ s ⁻¹	rms/μmol dm ⁻³	Flux/nmol m ⁻² s ⁻¹	Penetration depth/mm
D	Low	11.1	5.11	14	96	6.27
D	Low	21.8	9.02	11	129	4.77
D	Low	14.7	5.67	6	104	5.50
Mean	Low	15.9	6.60		110	5.51
E	Low	6.2	0.91	12	52	5.41
E	Low	3.3	0.58	13	43	6.03
E	Low	1.7	0.22	9	36	6.72
Mean	Low	3.7	0.57		44	6.05
C	Low	2.5	0.17	37	13	9.10
C	Low	3.3	0.17	14	12	11.02
C	Low	4.8	0.30	17	16	9.93
Mean	Low	3.5	0.21		14	10.02
D	High	14.5	4.69	19	93	5.82
D	High	14.3	3.47	27	88	5.81
Mean	High	14.4	4.08		91	5.82
E	High	3.7	0.33	10	35	7.90
E	High	7.3	0.65	16	45	6.21
Mean	High	5.5	0.49		40	7.06
C	High	6.8	0.36	21	17	10.63
C	High	4.6	0.14	41	13	6.77
Mean	High	5.7	0.25		15	8.70

Table 4. Sediment characteristics

Sediment code	Sediment layer/mm	Σ/m ² g ⁻¹	OM/%	Porosity
C	0–2	0.90	7.6	0.43
C	2–4	0.86	5.3	0.44
D	0–2	9.58	17.7	0.96
D	2–4	9.75	18.0	0.89
E	0–2	3.52	0.95	0.87
E	2–4	3.09	0.89	0.76

(1994). Previous research by Mackenthun and Stefan (1998) using a fluvium channel, has shown that the SOD depends on water velocity up to a limiting value depending on factors such as the reaction rates and sediment characteristics. For lake sediment, they found a velocity dependence between 0 and 3 cm s⁻¹ with no increase in SOD between 3 and 7 cm s⁻¹ but for sawdust, they found a dependence with velocity up to 10 cm s⁻¹. The present results are consistent with those from

the lake sediment with no velocity effect on the DO flux for river sediments at velocities between 10 and 20 cm s⁻¹ suggesting that reactions in the sediment are rate limiting rather than the diffusion of oxygen across the interface.

The rate constants show a linear increase with organic matter content ($r^2 = 0.80$, $n = 15$) and slightly improved correlation with the product of the specific surface area and organic matter content ($r^2 = 0.84$, $n = 15$). However, the reaction rate for the mixed sediment (E) was lower than calculated from the mixing ratio. The penetration depth increased with decreasing amount of organic matter (Table 3) and a regression according to Equation (11) produced a poorer correlation than previously (Figure 5b).

A more detailed examination of the changes in DO at the interface (Figure 6) reveals that only the fine sediment (D) gave evidence of a Diffuse Boundary Layer (DBL) discussed by Jorgensen and Revsbech (1985). This was estimated as 0.27 ± 0.18 mm for the low velocity and 0.16 (n = 2) for the high velocity, which are similar to the DBL thickness of 0.16 mm at 7.7 cm s⁻¹, measured above a microbial mat (Jorgensen and Marais 1990). However, for the coarser sediments, there was no evidence of a diffuse layer. The profile for sediment C indicated that the DO concentration remained at saturation for up to 1 mm below the point marked as the surface. This reflects the topography at the surface with coarser material in Sediment C producing an irregular interface and also reflects the method of locating the surface of the sediment, i.e. the first point of contact of the microelectrode tip with particles at the surface. Sand particles up to 2 mm in diameter located at the interface, protrude into the flow whereas in the finer sediment, the surface is closer to planar with the larger particles submersed in the majority of the silt fraction. The same changes in profile were found for the experiments at both velocities indicating the effect was not detectably influenced by advection of water into the sediment but by the irregular nature of the interface of the three sediments. As no DBL was detected in sediments C and E, the transport of DO is limited by oxidation reactions in the sediment and not diffusion through the boundary layer, as found for the organic rich sediment (D). This is consistent with the lower fluxes of *ca* 40 and 15 nmol m⁻² s⁻¹ for the two coarser sediments compared with *ca* 100 nmol m⁻¹ s⁻¹ for the silt sediment (Table 3). However, the existence of a DBL for sediment D does not cause a measurable effect of water velocity on the DO flux.

Conclusions

There are no measurements of dissolved oxygen concentration changes in river sediments in the literature although many have been reported for marine sediments and biofilm mats. The application of various models to describe the vertical DO profile in sediments gave best agreement with oxidation described by zero-order kinetics (with respect to DO concentration) and the Monod equation. Temporal changes in the DO profiles that developed in a bed-sediment showed that after mixing a sediment, although a steady-state DO profile was expected within < 1 h,

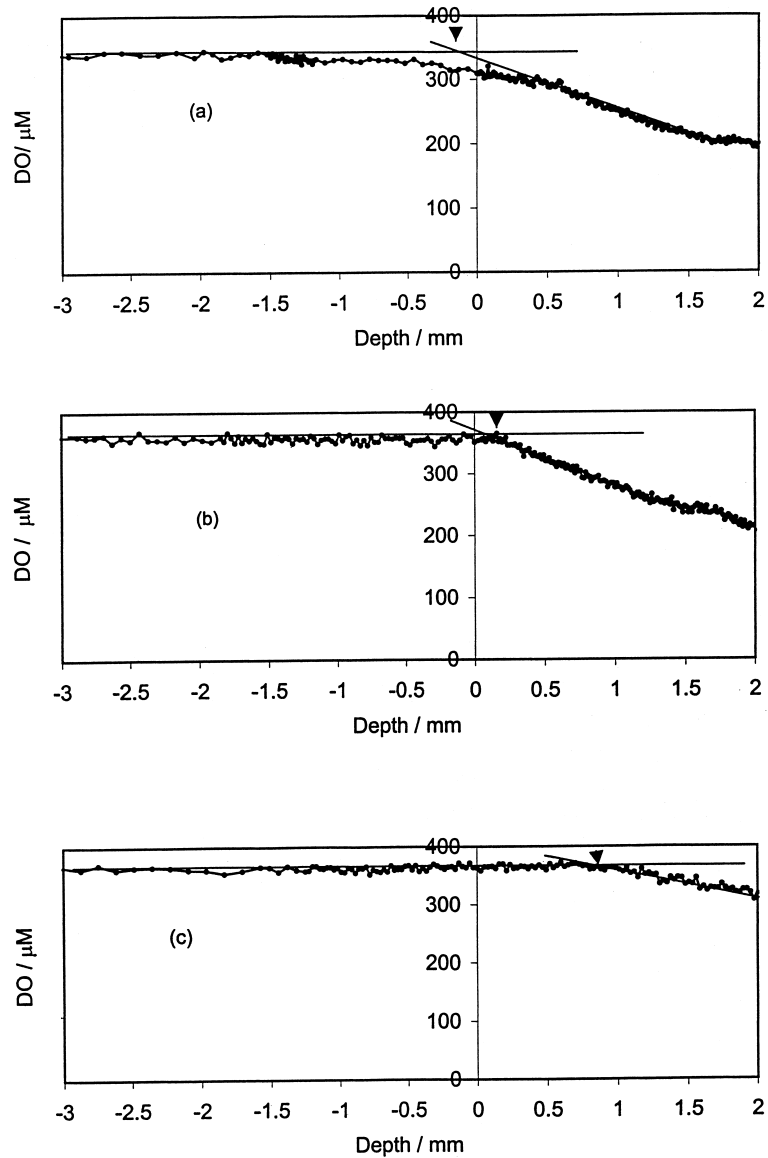


Figure 6. Changes in the DO profile measure at the interface at low velocity (10 cm s^{-1}). The arrows indicate the position of the intersection of the lines through the bulk water concentration and the linear region of the concentration decrease in the sediment (a) Sediment D. (b) Sediment E. (c) Sediment C.

changes in the profile and derived rate constant and flux at the interface occurred over a period of 38 days. The penetration of oxygen increased with time, probably as a result of changes in the oxidation reactions or microbial community. A general agreement was found between the depth of penetration of oxygen and the inverse

of the flux at the interface as given in Equation (11). This is in accord with the results from continental marine sediments. It was also found that low densities of *oligochaete* worms had no detectable effect on the DO concentration profiles.

Measurements with three sediments of different organic matter content and particle size, showed that the rate constant for the reaction of oxygen increased with organic matter content and the specific surface area of the sediments. The results at two velocities of water-flow (10 and 20 cm s⁻¹) concluded that there was no detectable effect on the DO flux at the interface or the computed rate constant. As no viscous or diffuse boundary layer was detected for either of the coarse sediments, it is surmised that the rate limiting steps in the transport process are the reactions in the sediment rather than diffusion across the boundary layer. As many river sediments are relatively coarse, it is difficult to define a "surface layer" through electrode profiles as sand particles of 1–2 mm size may protrude into the flowing water and make contact with the microelectrode tip.

Acknowledgements

I thank Frank Denison for help with some of the microelectrode measurements and Ian Allan for the study using benthic invertebrates. I acknowledge the support of NERC for this work.

References

- Allan I.J., House W.A., Warren N., Parker A. and Carter J.E. 2001. A Pilot Study of the Movement of Permethrin into Freshwater Sediments. Symposium Proceedings No. 78. British Crop Protection Council, Brighton, pp. 107–112.
- Benson B.B. and Krause D. Jr 1980. The concentration and isotopic fractionation of gases dissolved in freshwater in equilibrium with the atmosphere. 1. Oxygen. *Limnol. Ocean.* 25: 662–671.
- Barcelona M.J. 1983. Sediment oxygen demand fractionation, kinetics and reduced chemical substances. *Water Res.* 17: 1081–1093.
- Berninger U.G. and Markus H. 1997. Impact of flow on oxygen dynamics in photosynthetically active sediments. *Aquatic Microbial Ecology* 12: 291–302.
- Boudreau B.P. 1997. *Diagenetic Models and Their Implementation*. Springer-Verlag, New York.
- Bouldin D.R. 1968. Models for describing the diffusion of oxygen and mobile constituents across the mud-water interface. *J. Ecol.* 56: 77–87.
- Bowman G.T. and Delfino J.J. 1980. Sediment oxygen demand techniques: A review and comparison of laboratory and *in situ* systems. *Water Res.* 14: 491–499.
- Cae W.-J. and Sayles F.L. 1996. Oxygen penetration depths and fluxes in marine sediments. *Mar. Chem.* 52: 123–131.
- Chen G.-H., Leong I.-M., Liu J. and Huang J.-C. 1999. Study of the oxygen uptake by tidal river sediment. *Wat. Res.* 33: 2905–2912.
- Edwards R.W. and Rolley H.L.J. 1965. Oxygen consumption of river muds. *J. Ecology* 53: 1–19.
- Han P. and Bartels D.M. 1996. Temperature dependence of oxygen diffusion in H₂O and D₂O. *J. Phys. Chem.* 100: 5597–5602.

- House W.A., Denison F.H., Smith J.T. and Armitage P.D. 1995. An investigation of the effects of water velocity on inorganic phosphorus influx to a sediment. *Environmental Pollution* 89: 263–273.
- House W.A., Denison F.H., Warwick M.S. and Zmud B.V. 2000. Dissolution of silica and the development of concentration profiles in freshwater sediments. *Applied Geochemistry* 15: 425–438.
- Jorgensen B.B. and Marais D.J.D. 1990. The diffusive boundary layer of sediments: Oxygen microgradients over a microbial mat. *Limnol. Oceanogr.* 35: 1343–1355.
- Jorgensen B.B. and Revsbech N.P. 1985. Diffusive boundary layers and the oxygen uptake of sediments and detritus. *Limnol. Oceanogr.* 30: 111–127.
- Josiam R. and Stefan H. 1999. Effect of flow velocity on sediment oxygen demand: Comparison of theory and experiment. *J. American Water Resources Assoc.* 35: 433–439.
- Jubb S., Guymer I., Licht G. and Prochnow J. 2001. Relating oxygen demand to flow: development of an *in situ* sediment oxygen demand measuring device. *Water Sci. Technol.* 43: 203–210.
- Llanso R.J. 1992. Effects of hypoxia on estuarine benthos: the lower Rappahannock River (Chesapeake Bay), a case study. *Estuarine Coastal Shelf Sci.* 35: 491–515.
- Mackenthun A.A. and Stefan H.G. 1998. Effect of flow velocity on sediment oxygen demand: experiments. *J. Environ. Eng.* 124: 222–230.
- Martin P., Goddeeris B. and Martens K. 1993. Oxygen concentration profiles in soft sediment of Lake Baikal (Russia) near the Selenga delta. *Freshwater Biol.* 29: 343–349.
- Nielson L.P., Christensen P.B., Revsbeck N.P. and Sorensen J. 1990. Denitrification and oxygen respiration in biofilms studied with a microsensor for nitrous oxide and oxygen. *Microbial. Ecol.* 19: 63–72.
- Nriagu O.J. and Dell C.I. 1974. Diagenetic formation of iron phosphates in recent lake sediments. *Amer. Mineral.* 59: 934–946.
- Pamatmat M.M. and Banse K. 1969. Oxygen consumption by the seabed. II *In situ* measurements to a depth of 180 m. *Limnol. Oceanogr.* 14: 250–259.
- Park S.S. and Jaffe P.R. 1999. A numerical model to estimate sediment oxygen levels and demand. *J. Environ. Quality* 28: 1219–1226.
- Revsbech N.P., Sorensen J. and Blackburn T.H. 1980. Distribution of oxygen in marine sediments measured with microelectrodes. *Limnol. Oceanogr.* 25: 403–411.
- Seiki T., Izawa H., Date E. and Sunahara H. 1994. Sediment oxygen demand in Hiroshima Bay. *Water Res.* 28: 385–393.
- Sincovec R.F. and Madsen N.K. 1975. Software for nonlinear partial differential equations. *ACM Trans. Math. Software* 1: 232–260.
- Thirkette K.M. and Barrett K.L. 1994. Relationship between sediment handling techniques and emergence success for the midge *Chironomus riparius*. *Proc. Brighton Crop Prot. Conf.- Pests and Diseases* 3: 1331–1336.
- Vink P.M. and Van der Zee S.E.A.T.M. 1977. Effect of oxygen status on pesticide transformation and sorption in undisturbed soil and lake sediments. *Environ. Toxicol. Chem.* 16: 608–616.
- Wersin P., Hohener P., Giovanoli R. and Stumm W. 1991. Early diagenetic influences on iron transformations in a fresh-water lake sediment. *Chem. Geol.* 90: 233–252.
- Woodruff S., House W.A., Callow M.E. and Leadbeater B.S.C. 1999. The effects of a developing biofilm on chemical changes across the sediment-water interface in a freshwater environment. *Intern. Review of Hydrobiol.* 84: 509–532.

